Progress In Electromagnetics Research M, Vol. 59, 45–54, 2017

Wide Slot Antenna with Y Shape Tuning Element for Wireless Applications

Bhupendra K. Shukla*, Nitesh Kashyap, and Rajendra K. Baghel

Abstract—A wide slot antenna with Y shape tuning element is presented for wireless applications (GSM 1800, WiMAX, PCS and ITM-2000). The proposed antenna is fabricated on an FR-4 substrate ($\tan(\delta) = 0.02$, $\varepsilon_r = 4.3$) with the thickness of 1.6 mm. On the top layer of the substrate, a 50 ohm microstrip line is fabricated which is terminated in Y shape tuning element. On ground plane, an irregular wide slot and triangular notch are etched. In addition, for performance improvement two triangular shaped parasitic slots are embedded on the ground plane. The proposed antenna is energized by the microstrip line. It exhibited the bandwidth of 127.55% from 1.15 GHz to 5.2 GHz for $|S_{11}| < -10$ dB. Surface current distribution and radiation pattern at resonating frequencies 1.25, 1.9 and 4.2 GHz are analyzed. Impact of parameters on S_{11} characteristic is also studied to know the behavior of the antenna.

1. INTRODUCTION

Slot antennas are widely used in military, aircraft and many applications. These antennas possess various properties such as small volume, low cost, easy integration with microwave circuitry, facile fabrication and the ability to produce circular and linear polarization. The serious limitation of a narrow slot antenna is small bandwidth [1–3]. The bandwidth of an antenna is enhanced by incorporating slots on the ground plane and patch. These slots change the position of fundamental mode (TM_{10} or TM_{01}) and other higher order modes (TM_{12}, TM_{20}) or generate new resonance frequency near fundamental mode [4–6]. Creating a wide slot on the ground is another method to enhance impedance bandwidth of the antenna. Recently, many wide slot antennas have been reported for broadband applications such as rectangular slot [7, 8], triangular slot [9], rotated slot [10] and pentagonal slot [11]. The addition of tuning element with a proper dimension and location is another approach to improve the performance of a wide slot antenna. Some reported shapes of tuning elements are fork [12], U [13] and fractal [14]. Wide slot with the parasitic element is another technique to improve the performance of the antenna. In [15], two parasitic elements with rhombus slot were proposed that covered the bandwidth from 1.8 GHz to 6.09 GHz. In this communication, we propose a wide slot antenna with a Y shape tuning element for wireless applications (GSM 1800, WiMAX, PCS and ITM-2000). The proposed antenna covers the bandwidth of 127.55% from 1.15 GHz to 5.2 GHz for $|S_{11}| < -10$ dB. It is investigated on three stages both numerically and experimentally. In the first stage, a Y shape tuning element and wide slot ground are analyzed. Then, a triangular notch is embedded to improve the performance of antenna 1. On the final stage, two triangular slots are created at the corners of the ground plane. To observe the behaviour of the antenna, simulated current distribution and radiation patterns are also discussed.

Received 13 June 2017, Accepted 28 July 2017, Scheduled 3 August 2017
* Corresponding author: Bhupendra Kumar Shukla (bhupendrashuklaphd@gmail.com).
The authors are with the Maulana Azad National Institute of Technology, Bhopal, India.

2. ANTENNA GEOMETRY

The design and parameters of the proposed antenna are depicted in Figure 1. It is placed on the x-y plane, and the z-direction is normal to the Y shape tuning element. The proposed structure is fabricated on a fiberglass polymer resin (FR4) substrate with loss tangent ($\tan\delta$) $= 0.02$ and dielectric constant (ε_r) $= 4.3$. A $50\,\Omega$ microstrip line (M_1 (length of feed line) and M_2 (width of feed line)) is located on the top side of the substrate which is terminated in Y-shaped tuning element. On bottom side of the substrate, an irregular wide slot and a triangular notch are etched. In addition, to improve the performance of the antenna, two triangular parasitic slots are incorporated at the corners of the ground plane. The overall volume of the antenna is $70 \times 70 \times 1.6\,\text{mm}^3$. Optimized dimensions of proposed antenna are listed in Table 1.

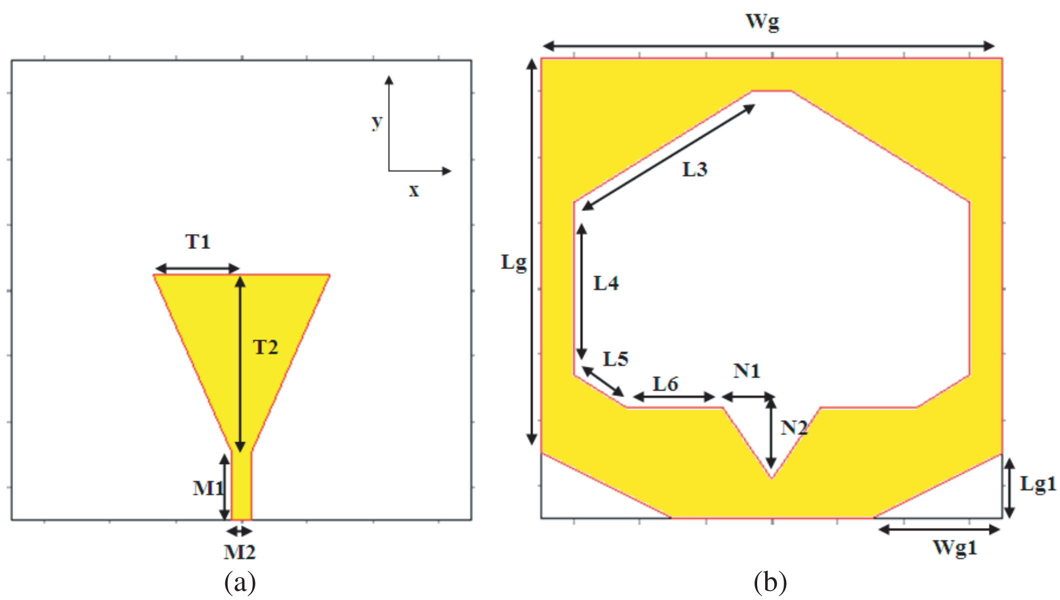

Figure 1. Geometry of proposed antenna. (a) Top view, (b) bottom view (yellow colour is metal).

Table 1. Optimized dimensions of proposed antenna.

Parameter	Dimension	Parameter	Dimension
M_1	7 mm	M_2	3 mm
T_1	13.5 mm	T_2	30.5 mm
W_g	70 mm	L_g	60 mm
L_{g1}	10 mm	W_{g1}	20 mm
N_2	11 mm	N_1	7.5 mm

3. RESULT AND DISCUSSION

The proposed wide slot antenna is investigated in three stages. Antennas 1, 2 and 3 are examined numerically using CST Microwave Studio. Further, the S_{11} characteristics and input impedance are measured using a vector network analyzer (N9923A). The prototypes of antennas 1, 2 and 3 are displayed in Figure 2. In stage 1, the performance of antenna 1 is analyzed without triangular notch and parasitic slots. Antenna 1 comprises an irregular wide slot and a 50 ohms feed line which is terminated in Y-shaped tuning stub. Comparison of simulated and measured S_{11} characteristics of antenna 1 are shown

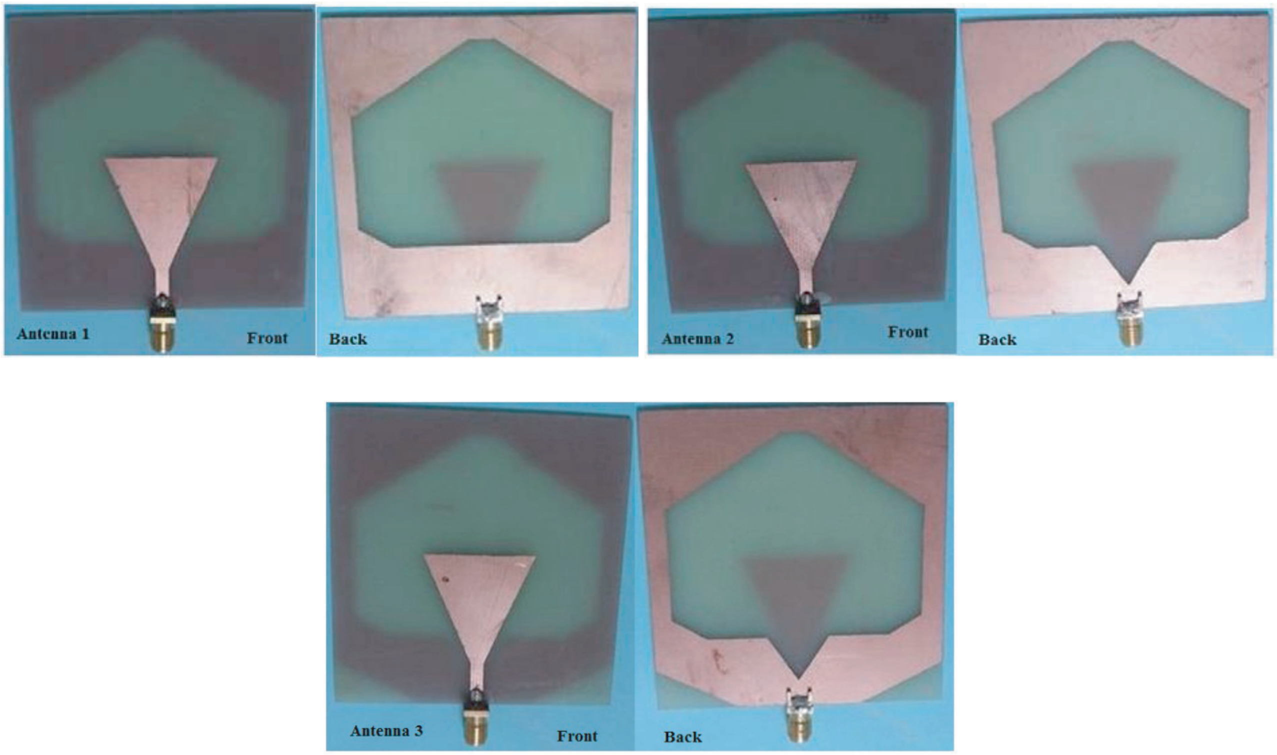

Figure 2. Prototypes of antenna 1, 2 and 3.

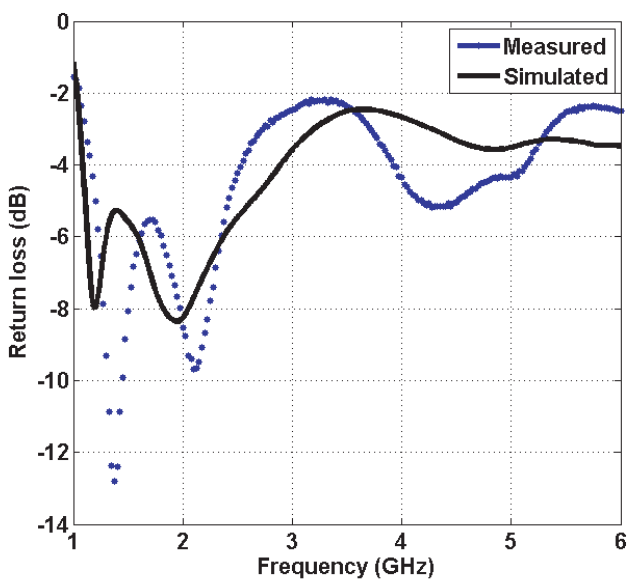

Figure 3. Measured and simulated return loss antenna 1.

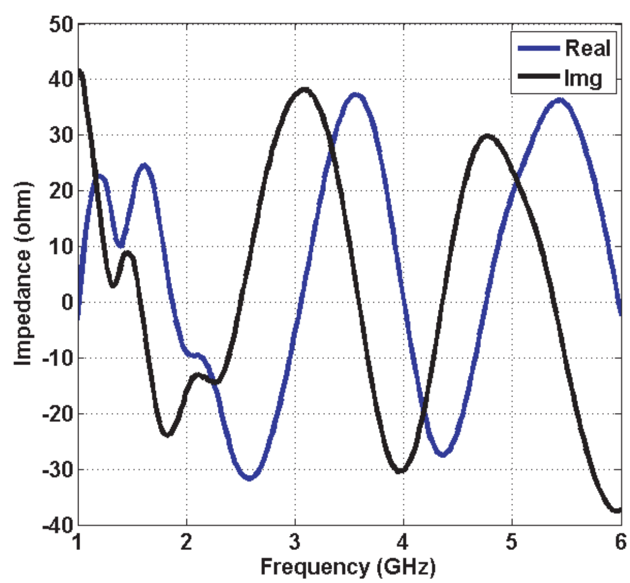

Figure 4. Measured input impedance of antenna 1.

in Figure 3. This antenna covers the frequency range from 1.33 GHz to 1.43 GHz (fractional bandwidth of 7.24%) for $|S_{11}| < -10$ dB. Poor impedance matching is found in the entire operating frequency band (1 to 6 GHz) except frequency band from 1.33 GHz to 1.43 GHz. The input impedance characteristic of antenna 1 is shown in Figure 4. The real and imaginary parts of the input impedance fluctuate between -40 and 40 ohm. In stage two, the return loss characteristics and impedance of antenna 2 are investigated. In antenna 2, a triangular notch is incorporated on the periphery of the wide slot, and rest of the geometry of antenna 2 is the same as antenna 1. The frequency response of antenna 2 is shown in Figure 5. It exhibits the bandwidth of 127.55% from 1.15 GHz to 5.2 GHz for $|S_{11}| < -10$ dB with one notched frequency band from 3.1 GHz to 3.73 GHz. A positive impact of triangular notch is observed. This triangular notch introduces the capacitive effect and improves the impedance matching level in the entire operating frequency band. Figure 6 shows the variation of the input impedance of antenna 2. The real and imaginary parts of the input impedance fluctuate between 20 and -25 ohm. In stage three, the performance of antenna 3 (proposed antenna) is analyzed. In antenna 3, two additional

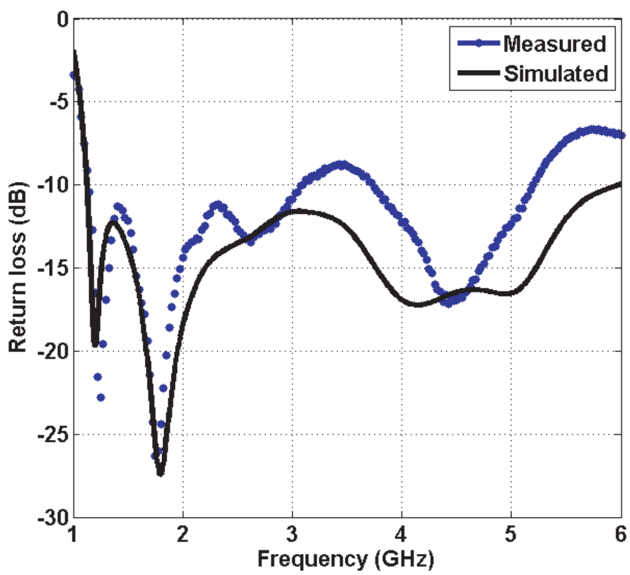

Figure 5. Measured and simulated return loss antenna 2.

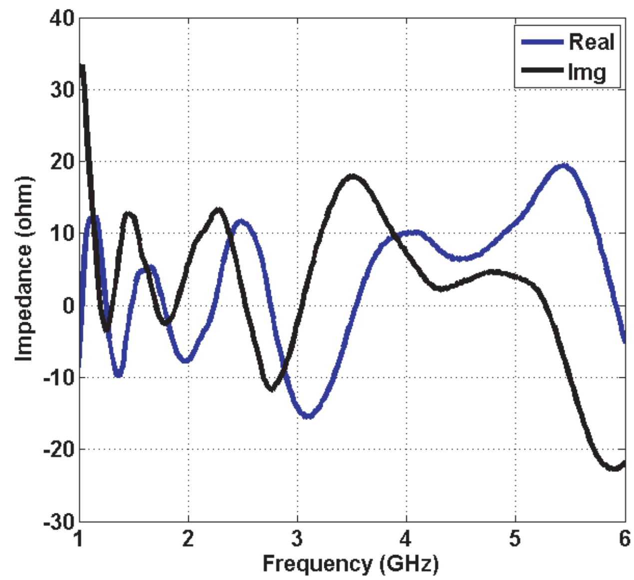

Figure 6. Measured input impedance of antenna 2.

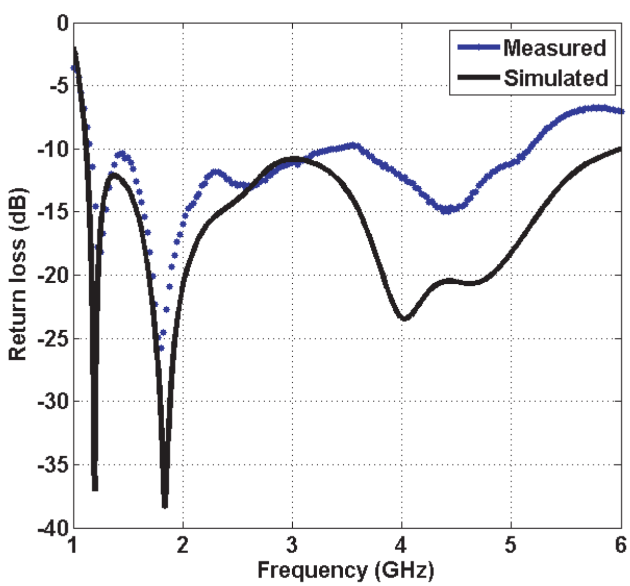

Figure 7. Measured and simulated return loss antenna 3.

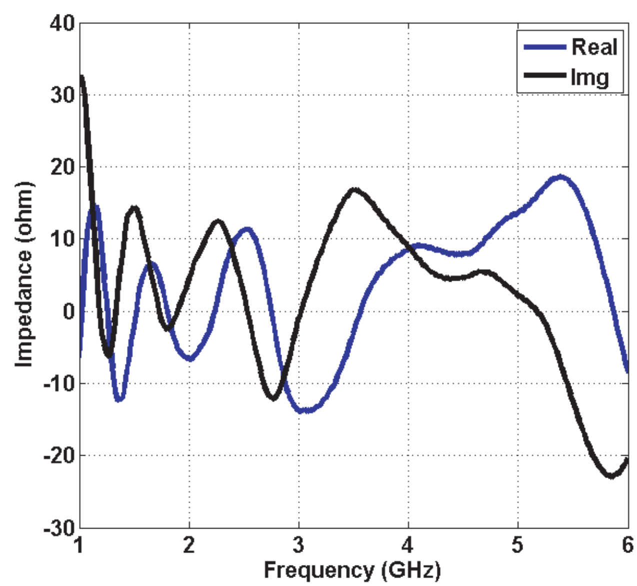

Figure 8. Measured input impedance of antenna 3.

triangular parasitic slots are created at the corners of the ground plane. These two parasitic slots improve the value of return loss at resonating frequencies and suppress the notch band from 3.1 GHz to 3.73 GHz. The $|S_{11}|$ characteristic of the proposed antenna (antenna 3) is shown in Figure 7. It covers a bandwidth of 127.55% from 1.15 GHz to 5.2 GHz for $|S_{11}| < -10$ dB. A good agreement between simulated and measured results is found. Figure 8 shows the variation of real and imaginary parts of the input impedance of antenna 3.

The current distributions at lower cutoff frequency (1.15 GHz) and other resonating frequencies (1.25, 1.9 and 4.2 GHz) are displayed in Figure 9. As depicted in Figure 9, current is distributed on the ground plane, along the periphery of the wide slot, length of the feed line and Y shape tuning element. It is found that the current distribution is symmetric about the longitudinal axis. At the lower cutoff frequency $f_l = 1.15$ GHz, current is distributed on the edge of the ground plane. This frequency is calculated by the following equations.

$$L = L_1 + L_2 + L_g + \frac{W_g}{2} \tag{1}$$

$$L_1 = \sqrt{\left(L_{g1}^2\right) + \left(W_{g1}^2\right)} \tag{2}$$

$$f_l = \frac{C}{L\sqrt{\varepsilon_r}} \tag{3}$$

where L is the length. The calculated lower cut-off frequency is 1.08 GHz. An error of 6.08% is

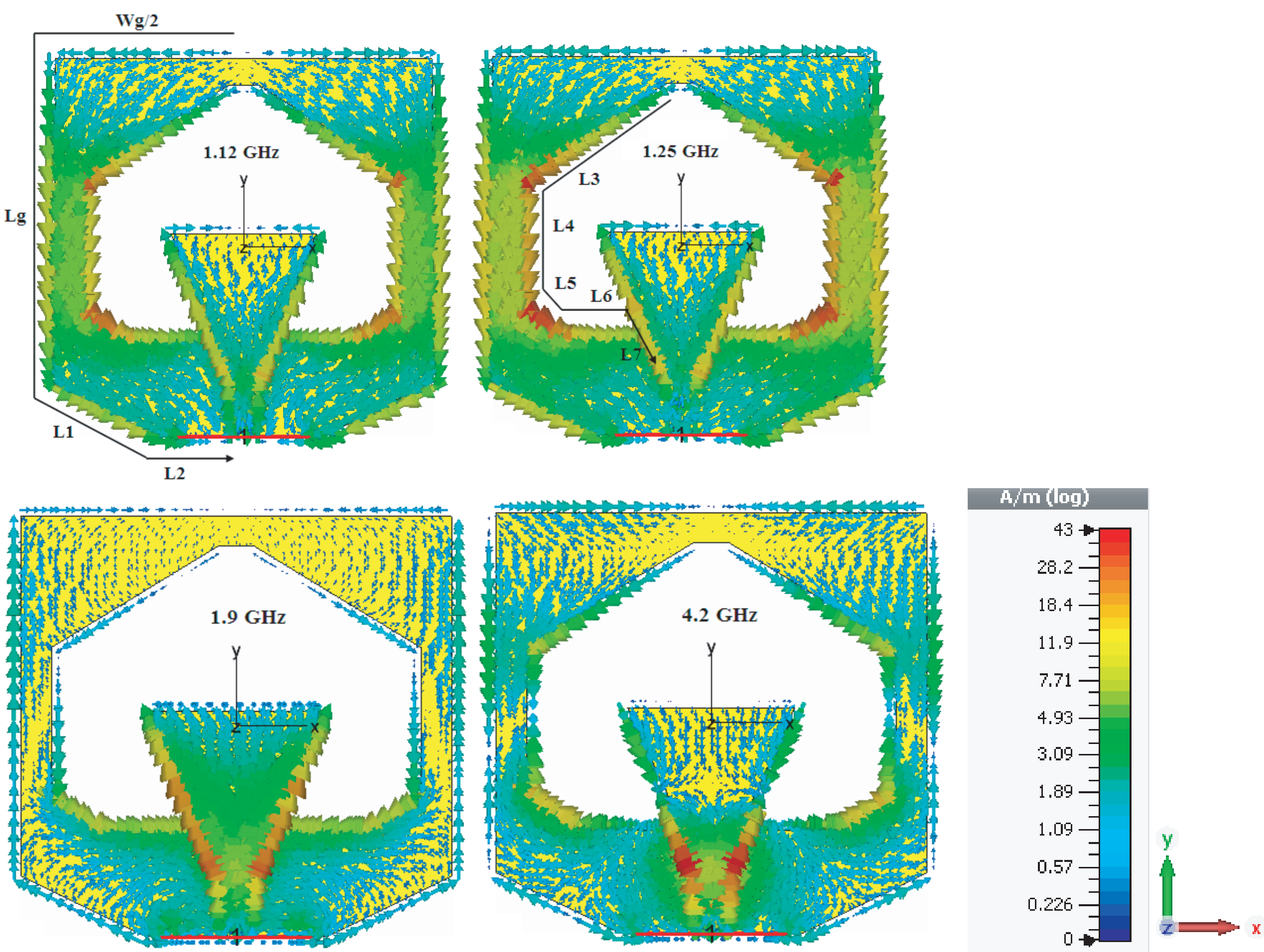

Figure 9. Surface current distributions of proposed antenna at the lower cut-off frequency and resonating frequencies.

calculated between simulated and calculated lower cutoff frequencies. At frequency 1.25 GHz, current is also distributed along the edge of the wide slot. The first resonance frequency f_1 is caused by the wide slot. It is calculated by following equations.

$$L_{first} = L_5 + L_6 + L_7 + L_3 + L_4 \tag{4}$$

$$L_7 = \sqrt{\left(N_1^2\right) + \left(N_2^2\right)} \tag{5}$$

$$f_1 = \frac{C}{L_{first}\sqrt{\varepsilon_r}} \tag{6}$$

The calculated first resonance frequency is 1.52 GHz. An error of 17.7% is found between simulated and calculated first resonance frequencies. At frequency 1.9 GHz, multiple half wave variation of current is found along the wide slot. No variations are investigated along the edges of the ground plane. At frequency 4.2 GHz, multiple half wave variation of current is found along the wide slot, edges of the ground plane and Y shape tuning element.

The far-field patterns of the proposed antenna at frequencies 1.25, 1.9 and 4.2 GHz are displayed in Figure 10. It is noticeable that the antenna exhibits bidirectional pattern in E-plane. The proposed antenna shows stable radiation pattern in E-plane. It is also clear from Figure 10 that the antenna shows omnidirectional pattern in H-plane except at frequency 4.2 GHz. At frequency 4.2 GHz, symmetry of the pattern is lost due to the presence of higher order modes. The simulated and measured gains of the proposed antenna at resonating frequencies are given in Table 2. Table 3 exhibits the comparison of the bandwidths of some reported slot antennas. As shown in Table 3, the proposed antenna offers larger impedance bandwidth than existing wide slot antennas [1, 5, 10, 12, 15]. It also occupies less volume than reported antenna [1, 12].

Table 2. Measured and simulated gains.

Operating frequency	Simulated gain (dB)	Measured gain (dB)
1.25	1.9	1.87
1.9	2.04	2.7
4.2	5	5.67

Table 3. Comparison of bandwidth and area of the different slot antenna.

Reference	f_l (GHz)	f_h (GHz)	BW (%)	Size (mm^2)
[1]	1.347	1.533	12.91	80×80
[5]	4.53	7.47	49	42×32
[10]	3.4	5.6	49.4	70×70
[12]	1.639	1.907	15.11	110×110
[15]	1.80	6.09	108.74	61×51.5
Proposed	1.15	5.2	127.55	70×70

4. PARAMETRIC STUDY

An impact of parameter $T1$ is displayed in Figure 11. $T1$ is varied from 12.5 to 14.5 mm. The position of resonance frequency f_2 and higher cutoff frequency f_h are altered with increasing the value of $T1$. Figure 12 exhibits the effect of parameter $T2$ on the frequency response of the antenna. Frequencies f_2 and f_h are shifted left with changing the value of $T2$ from 29.5 to 31.5 mm. It is also investigated from Figures 11 and 12 that parameters $T1$ and $T2$ change the impedance matching level on the entire

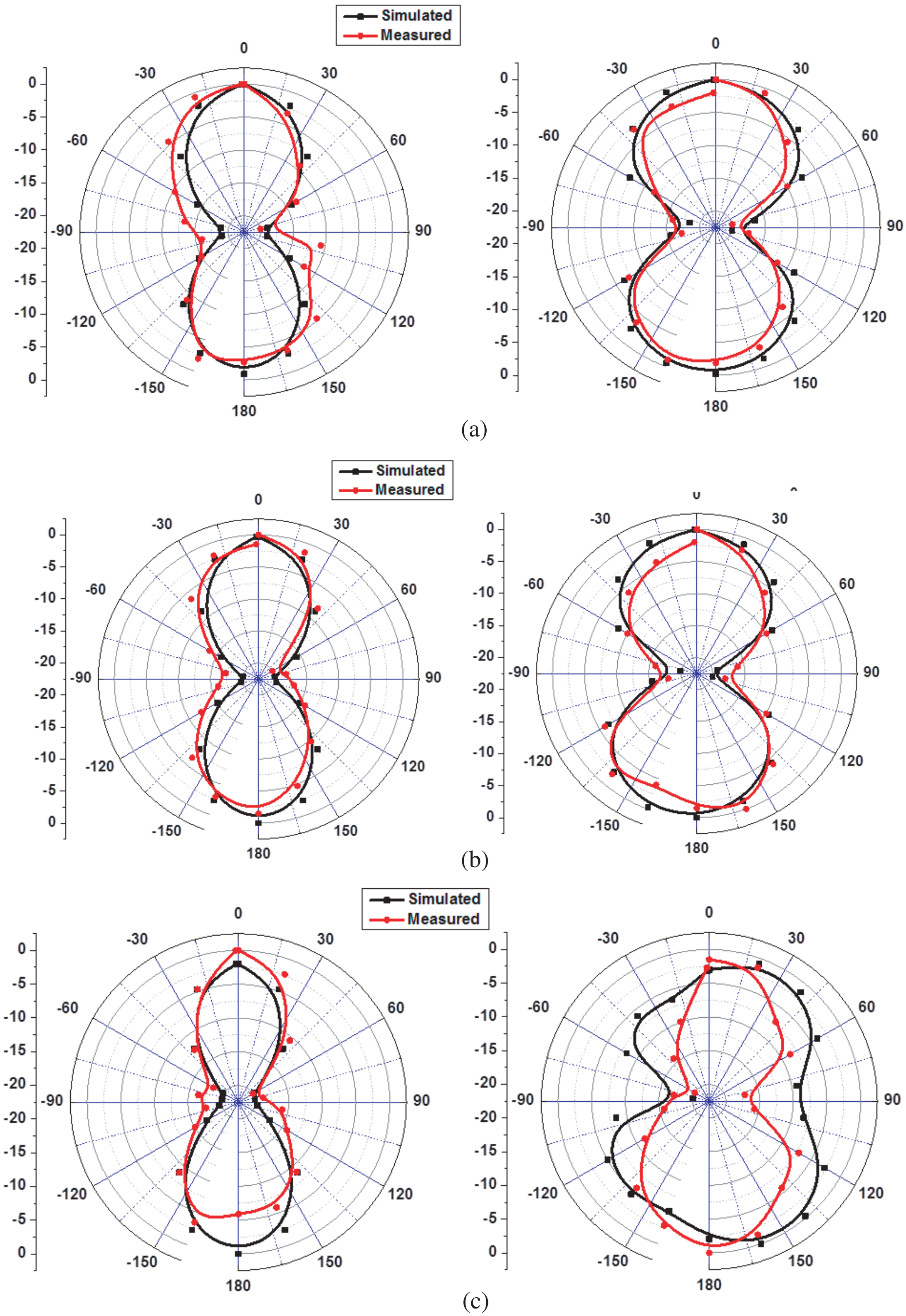

Figure 10. Far field patterns (E-plane (left), H-plane (right)) at frequencies (a) 1.25 GHz, (b) 1.9 GHz and (c) 4.2 GHz.

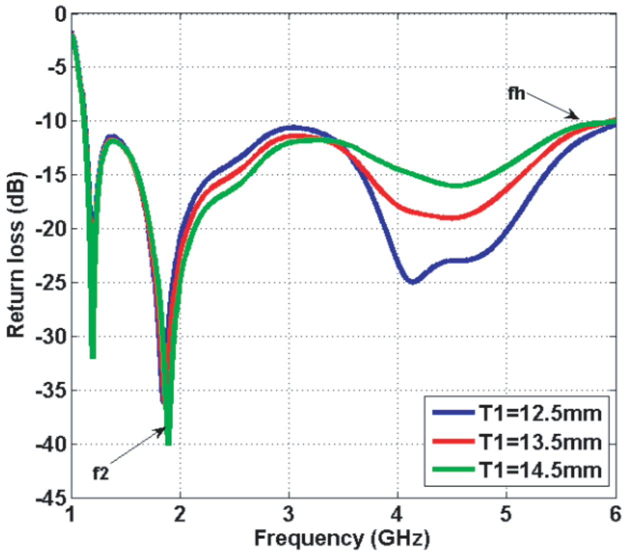

Figure 11. Effect of $T1$ on the frequency response of the antenna.

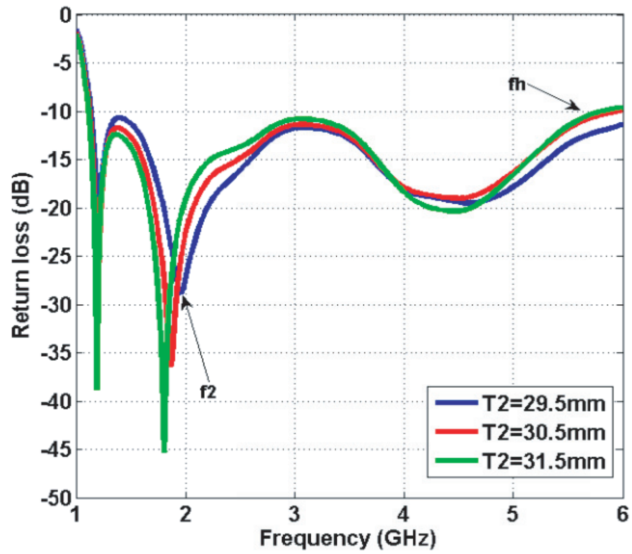

Figure 12. Effect of $T2$ on the frequency response of the antenna.

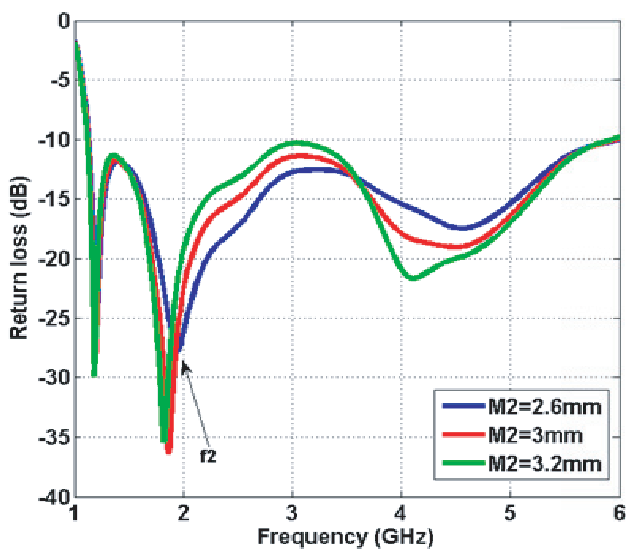

Figure 13. Effect of $M2$ on the frequency response of the antenna.

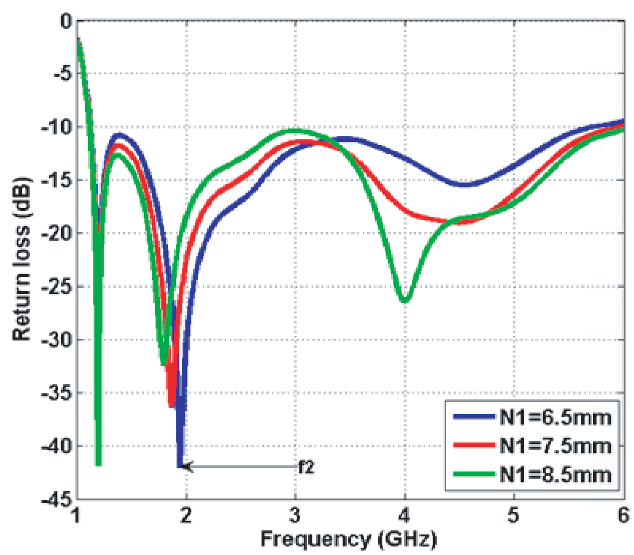

Figure 14. Effect of $N1$ on the frequency response of the antenna.

operating frequency band. The width of microstrip line $M2$ affects the frequency response of the antenna. Figure 13 shows the impact of $M2$. It is found that the impedance bandwidth of the antenna is decreased for $M2 > 3.2$ mm. Resonance frequency f_2 is shifted left with increasing the value of M2 from 2.6 to 3.2 mm.

The impact of parameter $N1$ is shown in Figure 14. Resonance frequency f_2 is shifted left by increasing the value of $N1$ from 6.5 to 8.5 mm. It is shown in Figure 14 that the impedance bandwidth is decreased for $N1 > 8.5$ mm. The effect of parameter $N2$ is exhibited in Figure 15. The value of $N2$ is varied from 9 to 11 mm. This parameter critically affects the bandwidth of the antenna. Maximum impedance bandwidth is found for $N2 = 10$ mm. For $N2 > 10mm$, the bandwidth of the antenna is decreased.

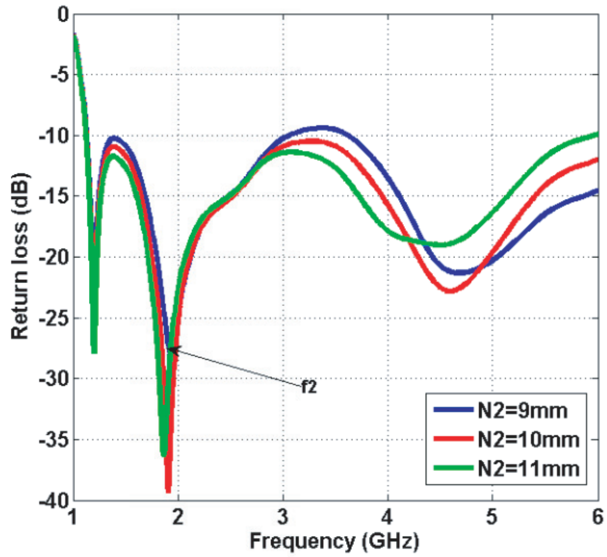

Figure 15. Effect of $N2$ on the frequency response of the antenna.

5. CONCLUSION

A wide slot antenna with Y shape tuning element has been verified for wireless applications (GSM 1800, WiMAX, PCS and ITM-2000). In this design, wideband performance is achieved by incorporating triangular notch and parasitic slots. The proposed antenna covers the bandwidth of 127.55% from 1.15 GHz to 5.2 GHz for $|S_{11}| < -10$ dB. The surface current distribution and far-field pattern at resonating frequencies (1.25, 1.9 and 4.2 GHz) are studied. Far-field pattern is found omnidirectional in H-plane and bidirectional in E-plane. The impact of parameters on frequency response of the antenna is also investigated. Parameters $N1$ and $N2$ affect the impedance bandwidth of the antenna.

REFERENCES

1. Wong, K. L., C. C. Huang, and W. S. Chen, "Printed ring slot antenna for circular polarization," *IEEE Transactions on Antennas and Propagation*, Vol. 50, 75–77, 2002.
2. Yoshimura, Y., "A microstripline slot antenna (short papers)," *IEEE Transactions on Microwave Theory and Techniques*, Vol. 20, 760–762, 1972.
3. Huang, J. F. and C. W. Kuo, "CPW-fed bow-tie slot antenna," *Microwave and Optical Technology Letters*, Vol. 19, 358–360, 1998.
4. Deshmukh, A. A. and K. P. Ray, "Formulation of resonance frequencies for dual-band slotted rectangular microstrip antennas," *IEEE Antennas and Propagation Magazine*, Vol. 54, 78–97, 2012.
5. Ansari, J. A., A. Singh, and M. Aneesh, "Desktop shaped broadband microstrip patch antennas for wireless communications," *Progress In Electromagnetics Research Letters*, Vol. 50, 13–18, 2014.
6. Deshmukh, A. A. and G. Kumar, "Broadband compact V-slot loaded RMSAs," *Electronics Letters*, Vol. 42, 1, 2006.
7. Jang, Y. W., "Broadband cross-shaped microstrip-fed slot antenna," *Electronics Letters*, Vol. 36, 2056–2057, 2000.
8. Jang, Y. W., "A circular microstrip-fed single-layer single-slot antenna for multi-band mobile communications," *Microwave and Optical Technology Letters*, Vol. 37, 59–62, 2003.
9. Shameena, V. A., S. Mridula, A. Pradeep, S. Jacob, A. O. Lindo, and P. Mohanan, "A compact CPW fed slot antenna for ultra wide band applications," *AEU-International Journal of Electronics and Communications*, Vol. 66, 189–194, 2012.

10. Jan, J. Y. and J. W. Su, "Bandwidth enhancement of a printed wide-slot antenna with a rotated slot," *IEEE Transactions on Antennas and Propagation*, Vol. 53, 2111–2114, 2005.
11. Shinde, P. N. and J. P. Shinde, "Design of compact pentagonal slot antenna with bandwidth enhancement for multiband wireless applications," *AEU-International Journal of Electronics and Communications* Vol. 69, 1489–1494, 2015.
12. Sze, J. Y. and K. L. Wong, "Bandwidth enhancement of a microstrip-line-fed printed wide-slot antenna," *IEEE Transactions on Antennas and Propagation*, Vol. 49, 1020–1024, 2001.
13. Javan, D. S., M. A. Salari, and O. H. Ghoochani, "Cross-slot antenna with U-shaped tuning stub for ultra-wideband applications," *International Journal of Antennas and Propagation*, 2008.
14. Lui, W. J., C. H. Cheng, Y. Cheng, and H. Zhu, "Frequency notched ultra-wideband microstrip slot antenna with fractal tuning stub," *Electronics Letters*, Vol. 41, 294–296, 2005.
15. Jan, J. Y. and L. C. Wang, "Printed wideband rhombus slot antenna with a pair of parasitic strips for multiband applications," *IEEE Transactions on Antennas and Propagation*, Vol. 57, 1267–1270, 2009.